Adsorption mechanisms of high-levels of ammonium onto natural and NaCl-modified zeolites

Lin Lin[a], Zhongfang Lei[a,b,*], Li Wang[a], Xiang Liu[a], Yi Zhang[a], Chun-Li Wan[a], Duu-Jong Lee[a], Joo Hwa Tay[a]

[a]Department of Environmental Science & Engineering, Fudan University, 220 Handan Road, Shanghai 200433, China

[b]Graduate School of Life and Environmental Sciences, University of Tsukuba, 1-1-1 Tennoidai, Tsukuba, Ibaraki 305-8572, Japan

*Corresponding author. Present address: Graduate School of Life and Environmental Sciences, University of Tsukuba, 1-1-1 Tennoidai, Tsukuba, Ibaraki 305-8572, Japan.

Email: zflei2005@yahoo.com.cn or lei.zhongfang.gu@u.tsukuba.ac.jp

Phone/Fax: +81 29 853 6703

Abstract

Zeolites, microporous aluminosilicate minerals, have high affinity to ammonium in water. This study explored the mechanisms of ammonium adsorption onto natural zeolite and NaCl-modified counterpart under different ammonium levels (10-4000 mg-N/L) and initial pH 3.4-11.1. Ion exchange dominated the ammonium adsorption process near neutral pH, with the order of exchange selectivity following $Na^+ > Ca^{2+} > K^+ > Mg^{2+}$. At high ammonium levels, Ca^{2+} exceeded Na^+ as the dominant ions for ammonium adsorption. Conversely, in strong alkaline solutions, molecular adsorption suppressed ion exchange in ammonium adsorption. NaCl modification effectively increased ammonium adsorption capacity by increasing the Na contents in zeolite and by modifying the surface morphology to enhance film mass transfer rate. The modified zeolite presents a potential adsorbent to reduce ammonium concentration in landfill leachates, livestock wastewaters or effluents from

anaerobic digestion tanks of livestock manure.

Keywords: Zeolite; ammonium; ion exchange; molecular adsorption; NaCl modification

1. Introduction

Zeolites are microporous aluminosilicate minerals which could be used as ion exchanger in domestic and commercial water purification, softening and other applications [1]. Substitution of silicon by aluminum atoms in the crystal framework leads to extra negative charge to be balanced by surrounding counterions (such as Na^+, K^+, Ca^{2+}, Mg^{2+}, etc), and these counterions are easily exchanged by other surrounding cations in a contact solution [2]. Additionally, the high ion exchange capacity (IEC) [3], large reserves of zeolite-rich rock, shortage of competing minerals and the relatively low market price prefer the use of zeolites in large scales.

There are more than 50 species of zeolites, such as clinoptilolite, heulandite, mordenite, erionite, and others[2]. Use of clinoptilolite in industry and academia mainly focuses on its ion exchange properties, especially on its high adsorption capacity and selectivity for ammonium (NH_4^+) [4] . Ames [5] noted that the ion exchanging selectivity of clinoptilolite followed $Cs^+> Rb^+> K^+> NH_4^+> Ba^{2+}> Sr^{2+}> Na^+> Ca^{2+}> Fe^{3+}> Al^{3+}> Mg^{2+} >Li^+$. Zeolite dosage, particle size, initial ammonium concentration, pH, and temperature could have significant effects on ammonium adsorption capacity [6,7]. Several modification methods have been tried to enhance the ammonium adsorption capacity of zeolite, including microwave pretreatment [8], NaOH, HCl or NaCl solution treatment [9], integrated calcination [10], and others. Equilibrium isotherm and kinetics models of ammonium adsorption onto zeolites were also reported [11,12]. Presence of competing cations, like Na^+, K^+, Ca^{2+} and Mg^{2+}, adversely affects ammonium adsorption capacity of zeolites [6].

Zeolites can provide adsorption sites with exchangeable cations for ammonium ion and porosity for free ammonia [13], with ion exchange and molecular adsorption being the main

2

mechanisms, respectively. Although the latter is in significant importance especially in practice due to various pH feeds needed to deal with, few reports could be found on the contribution of molecular adsorption to the whole process. In addition, landfill leachates, livestock wastewater, and effluents from anaerobic digestion tanks of livestock manure could contain ammonium greater than 1000 mg-N/L [14-16]. However, current studies on ammonium adsorption onto zeolite are usually conducted at low ammonium levels (<1000 mg-N/L) [6-8, 17].

The objective of this study was to investigate the mechanisms for ammonium adsorption onto zeolite at ammonium concentration of 10-4000 mg-N/L. Contributions of ion exchange and molecular adsorption mechanisms during ammonium adsorption onto zeolite were clarified. Effects of ammonium concentration and solution pH (3.4-11.1) on adsorption behavior were discussed. Accordingly, we identified the rate-limiting steps for adsorption kinetics on natural and modified zeolites. To be specific, the term ammonium is the sum of free ammonia (NH_3) and ionized ammonium (NH_4^+).

2. Materials and methods

2.1. Materials

Two kinds of zeolites were used in this study. One is natural zeolite which was obtained from Shenshi Mine located in Jinyun, Zhejiang Province, China, and was prepared through crushing, sieving (1.43–0.80 mm), washing with deionized water and air-drying at $105 \pm 1\,℃$ for 6 hours. Another is modified zeolite which was obtained by immersing 5 g of natural zeolite in the flask containing 100 mL of 2 mol/L sodium chloride (NaCl) solution under $35 \pm 1\,℃$ and 100 rpm in a thermostatic shaker (HZQ-X3000, China) for 24 hours, and then washed with deionized water for three times and dried at $105 \pm 1\,℃$ for 6 hours.

The feed solutions were prepared by diluting 4000mg-N/L of ammonium chloride (NH_4Cl) stock solution with deionized water. All chemicals were of analytical grade, and deionized

water was used throughout the experiments.

2.2. Experimental methods

For each batch adsorption experiment, 2 g of zeolite was firstly added into the flask containing 100mL of a prescribed initial concentration of NH_4^+ solution at desired pH level (adjusted using 0.1mol/L HCl or NaOH solution). Then the flask was shaken at specified agitation speed and temperature controlled in the thermostatic shaker (HZQ-X3000, China). The suspension was finally filtered via 0.45 μm filter and the filtrate was analyzed for the target compound(s).

The agitation speed, temperature, initial ammonium concentration, pH, and contact time were the operational parameters investigated in this test. Table 1 lists the detailed conditions for each experiment.

The adsorption performance was evaluated by the amount of ammonium absorbed on per unit mass of zeolite (q in mg-N/g), which could be calculated according to Eq. (1).

$$q=(C_0-C_e)V/m \tag{1}$$

where C_o and C_e are the initial and equilibrium ammonium concentrations (mg-N/L), respectively. V is the ammonium solution volume (L) and m is the mass of zeolite used (g).

2.3. Analytical methods

Identification of mineral species of the zeolites was carried out by X-ray diffraction (XRD, Bruker-D8 Advance, USA) of the random-oriented powder samples. Energy disperses X-ray spectroscopy (EDS, EDAX-TEAM^{TM} EDS, USA) was used to determine the chemical composition of samples. The surface morphology of the zeolites was observed by scanning electron microscope (SEM, Philips-XL30 Electron Microscope, Netherland). The BET specific surface area, pore volume and diameter of zeolite samples were determined at P/P_0 ≥0.995 by nitrogen gas adsorption analyzer (Micromeretics-Tristar 3000, USA).

The concentrations of Na^+, K^+, Ca^{2+} and Mg^{2+} in solution were measured by atomic

absorption spectroscopy (AAS, Hitachi-Z 5000, Japan). The concentration of ammonium in solution was determined with the Neslerization method [18]. The solution pH was determined by a pH Meter (Hach-HQ11d, USA). All tests were done in duplicate with average data reported.

3. Results and discussion

3.1. Adsorbent characterization

The XRD patterns of the natural and modified zeolites revealed that the main mineral species in the natural zeolite were clinoptilolite-Na (formula: $(NaKCa)_5Al_6Si_{30}O_{72}\cdot18H_2O$), heulandite (formula: $Ca_{3.6}K_{0.8}Al_{8.8}Si_{27.4}O_{72}\cdot26.1H_2O$) and quartz (formula: SiO_2) (Fig. 1), accounting for 48%, 40% and 10%, respectively. The intensity changes of XRD peaks for the natural and modified zeolites indicated that the crystal frame structure of zeolite was intact after NaCl modification. However, the contents of quartz and heulandite seemed decreasing while clinoptilolite-Na increasing after NaCl modification. This observation may be a consequence of cation exchange (K^+, Ca^{2+} and Mg^{2+}) with Na^+, correlating with the EDS results (Table 2). In particular, the Na content increased by 192%, while Ca, Mg and K contents decreased by 78%, 60% and 26% respectively after NaCl modification.

Besides, the surface of modified zeolite became rougher and more irregular compared with the original zeolite (Figs. 2(a) and 2(b)). And the BET surface area, total pore volume, and average pore diameter of zeolite were significantly increased after NaCl modification (Table 3). The results indicate that NaCl immersion is an effective means to modify the surface of present zeolite samples.

3.2. Effects of agitation speed and temperature

Agitation speed had no noticeable effects on ammonium adsorption capacity after 24 hours testing, but it had great impact on adsorption kinetics, especially during the initial 120 min of testing (Fig. 3(a)). Specifically, the ammonium adsorption rate increased from 0.049

mg-N/(g·min) to 0.066 mg-N/(g·min) when agitation speed was increased from 0 to 100 rpm with the increasing trend leveled off at higher agitation speeds. Restated, the external mass transfer resistance from bulk solution to zeolite surface was diminished at >100 rpm agitation speed [7]. This observation indicated that the adsorption was not equilibrated with ion transfer rates at external boundary layers, and the role of surface reaction dominated the process. The results were in accordance with the findings of Erdogan and Ulku [7] and Alkan, et al. [19].

Figure 3(b) showed the effect of temperature on ammonium adsorption by natural zeolite. It seemed that the equilibrium adsorption capacity was not distinctively improved by increasing temperature from 25 to 45 ℃. Probably during this process the effective adsorption sites on the zeolite remained unchanged, although ammonium diffusion process may be promoted under higher temperature conditions in which ammonium moves more quickly in solution[19], water viscosity decreases [20], and adsorption sites on the zeolite become more energetic.

Based on the above results, the following experiments were carried out under the condition of 100 rpm and 35℃.

3.3. Mechanisms of ammonium adsorption onto zeolite

3.3.1. Adsorption isotherm

Adsorption isotherms can be used to reveal how ammonium ions interact with zeolite surfaces [21]. Langmuir isotherm is applied in this study to describe the monolayer adsorption onto the surface of adsorbent, assuming that the number of energetic adsorption sites are homogeneous and can be saturated [11]:

$$q = q_{max}K_LC_e/(1+K_LC_e) \qquad\qquad (2)$$

where q_{max} (mg-N/L) and K_L (L/mg) are the maximum ammonium adsorption capacity and the equilibrium constant, respectively. C_e (mg-N/L) and q (mg-N/g) represent the ammonium concentration in the solution and ammonium adsorption capacity at equilibrium, respectively.

The linearisation of Eq. (2) is given by Eq. (3)

$$C_e/q=1/(K_Lq_{max})+C_e/q_{max} \qquad (3)$$

The Freundlich isotherm assumes that the adsorbent has a heterogeneous surface with non-uniform distribution of adsorption sites. Freundlich parameters can be determined by Eq. (4) [11]

$$q=K_FC_e^{1/n} \qquad (4)$$

where K_F and $1/n$ represent the Freundlich capacity coefficient and the Freundlich intensity parameter, respectively. The linearisation of Eq. (4) is Eq. (5)

$$logq=logK_F+1/n \, logC_e \qquad (5)$$

The parameters for the Langmuir and Freundlich isotherms were evaluated based on the data from present experimental ammonium-zeolite systems (Table 4), with the Langmuir fitting the data better than the Freundlich. This implies that ammonium adsorption onto the natural zeolite is more like a monolayer adsorption process with uniform distribution of energetic adsorption sites on its surface. The maximum adsorption capacity of the natural zeolite was estimated 14.3 mg-N/g, slightly higher than those of Yusof et al. [22] (11.3 mg-N/g for granulated natural Indonesian mordenite), of Karadag et al. [17] (6.32 mg-N/g for Turkish clinoptilolite), and of Widiastuti et al. [12] (3.89 mg-N/g for Australian natural zeolite).

3.3.2. Ion exchange

According to the fundamental of ion exchange between solid and liquid phases [23], the ion exchange process between zeolite frame and aqueous ammonium solution can be expressed by Eq. (6)

$$Ze\text{-}M^{n+}+nNH_4^+ \longleftrightarrow Ze\text{-}nNH_4^++M^{n+} \qquad (6)$$

where Ze and M represent zeolite and the loosely held cations in zeolite, respectively, and n is the number of electric charge.

Assuming that the exchangeable cations in zeolites are Ca^{2+}, Na^+, K^+ and Mg^{2+} [24], the

ion exchange capacity (IEC) is defined as the sum of exchanged cations as follows:

$$IEC=[Na^+]+[K^+]+2[Ca^{2+}]+2[Mg^{2+}]=[NH_4^+] \tag{7}$$

Figure 4 shows the variation of equivalent concentrations of Ca^{2+}, Na^+, K^+, and Mg^{2+} released into solution under different initial ammonium concentrations. The sum of these four cations (IEC) was almost equal to the ammonium adsorption capacity at equilibrium (q), demonstrating the predominant role of ion exchange in ammonium adsorption to zeolite. The maximum IEC was 0.92 meq/g, lower than the theoretical ion exchange capacity (TIEC) [24], 2.86 meq/g from chemical composition of natural zeolite if all alkaline and alkaline-earth cations in zeolite were replaced. Restated, about 32% of the exchangeable sites were available for ammonium adsorption, probably owing to limited access of ammonium ions to interior sites of zeolites.

From Fig. 4, the order of ammonium ion exchange selectivity for cations on the natural zeolite was determined as $Na^+ > Ca^{2+} > K^+ > Mg^{2+}$, slightly different from results of Watanabe et al. [25] ($Na^+ >> K^+ > Ca^{2+} > Mg^{2+}$). This inconsistency is attributed to the difference in chemical compositions of tested zeolites: rather low Ca content in their chosen zeolite. Na^+ was the dominant cation exchanged with ammonium under lower initial ammonium concentration conditions (less than 500mg-N/L) (Fig. 4). With the increase of initial ammonium concentration Ca^{2+} started to dominate the ion exchange process after most Na being released, especially at higher initial ammonium concentrations (> 1000 mg-N/L). Conversely, K^+ is preferred than NH_4^+ in ion exchange sequence for clinoptilolite [[5]. In the present tests the K^+ was low in concentration and was slightly increased with initial ammonium concentration. Owing to the strong affinity of K^+ with zeolite, K^+ released by ammonium adsorption might be re-adsorbed back to zeolite via exchange with Na^+, Ca^{2+} or Mg^{2+}. After most available sites were covered by ammonium ions, the released K^+ could not be easily re-adsorbed back so its concentration was increased in solution. The low content in zeolite and high hydrated radius in solution hindered the exchange of Mg^{2+} with ammonium ions [26].

The ion exchange mechanism of ammonium adsorption could be confirmed by comparing chemical composition changes of natural zeolite before and after adsorption (Table 2). Clearly at 1000mg-N/L of ammonium the contents of Na, Ca, K, and Mg of the natural zeolite decreased after reaching the equilibrium of ammonium adsorption.

3.3.3. *Molecular adsorption*

Ammonium in the bulk solution exists in both ionized and molecular forms. pH and temperature affect the forms of ammonium in solution [27]. The relationship between pH, temperature (T), ionized ammonium (NH_4^+-N), free ammonia (NH_3-N) and total ammonium (TAN) can be expressed by Eqs. (8)-(10) [27]

$$[NH_3\text{-}N](mg/L)/[TAN](mg/L)=10^{pH}/(10^{pH}+e^{6344(273+T)}) \qquad (8)$$

$$[NH_4^+\text{-}N](mg/L)/[TAN](mg/L)=e^{6344(273+T)}/(10^{pH}+e^{6344(273+T)}) \qquad (9)$$

$$[TAN]=[NH_3\text{-}N]+[NH_4^+\text{-}N] \qquad (10)$$

The distributions of the free and ionized forms of ammonium were calculated based on Eqs. (8)-(10) at 100 mg-N/L and 1000 mg-N/L of initial ammonium concentrations (35℃). When pH<7, more than 95% of the ammonium existed in ionized form (NH_4^+); when pH approached 11, only about 1% of ammonium was left in ionized form(data not shown).

Figure 5 depicts that the ammonium adsorption onto natural zeolite is a pH-dependent process. The maximum ammonium removal occurred at pH 6.4 or 6.5, about 82.3 mg-N/L and 215.8 mg-N/L for 100 mg-N/L and 1000 mg-N/L of initial ammonium concentrations, respectively. The ammonium removal decreased slightly with decreasing pH, principally being attributed to the increase in competing hydrogen ions. The increase in pH reduced ammonium removal, especially at pH>9, likely owing to the fewer ammonium ions presented in alkaline solutions. This observation correlates with the findings by Huang et al.[6] and Erdogan and Ulku[7].

The increase in ammonia removal at increased pH and initial ammonia concentration suggests the interplay of molecular adsorption mechanism. The significance of molecular adsorption was negligible at pH<8. At pH 9.5, 45% and 8.5% of ammonium removal were contributed by free ammonia adsorption under 100 mg-N/L and 1000 mg-N/L, respectively (Figs. 5(a) and 5(b)). At pH 11.1, molecular adsorption was the dominant mechanism owing to the absence of ionized ammonium in solution (Fig. 5). Anyway, the molecular adsorption was of secondary importance and contributed less to the total ammonium removal according to the experimental results under neutral pH conditions.

3.4. Kinetic analysis

Figure 6 illustrates the kinetic data for natural and modified zeolites at 1000 mg-N/L of initial ammonium concentration. Ammonium adsorption on zeolite proceeded fast, particularly during the initial 100 min of testing, which might be a result of vacant adsorption sites on the zeolites [28]. The equilibrium could be reached in 12 hours (Fig. 6(a)).

Compared with the natural zeolite, the modified zeolite exhibited 58% higher in ammonium adsorption capacity and at faster adsorption rate, especially during the first 15 min of adsorption. This observation is attributable to the higher Na ions for modified zeolite than the original zeolite, and the absorbed Na^+ ions were readily exchanged by ammonium ions on zeolite surfaces. This statement was manifested by the result from AAS analysis showing that about 95% of IEC was Na^+ under 1000 mg-N/L of ammonium for modified zeolite (data not shown). Additionally, NaCl modification replaced Ca and Mg on zeolite resulting in producing large pores and cavities in the zeolite (Table 3 and Fig. 2). So the modified zeolite could have superior adsorption performance than the original zeolite.

Intra-particle diffusion model can be adopted to identify the diffusion mechanism of ammonium adsorption process [29]

$$q_t = k_d \, t^{1/2} + C \qquad\qquad\qquad\qquad (11)$$

where k_d is the coefficient of intra-particle diffusion ($mg/(g \cdot min^{1/2})$).

Figure 6(b) depicts that the intra-particle diffusion model fitted well the experimental data if the whole adsorption process was divided into two linear regions. Hence, the ammonium adsorption process might be described by film diffusion followed by intra-particle diffusion process[30]. The contribution of each rate controlling step in the ammonium adsorption onto zeolite was further analyzed by calculating the film diffusion (D_f) and particle diffusion (D_p) coefficients according to the corresponding models given below[20,23]:

Film diffusion model:

$$\ln(1 - q_t/q_e) = -k_f \, t \qquad\qquad\qquad\qquad (12)$$

Particle diffusion model:

$$\ln[1 - (q_t/q_e)^2] = -2k_p \, t \qquad\qquad\qquad\qquad (13)$$

where $k_f = D_f C_s/C_z hr$ and $k_p = D_p \pi^2/r^2$ are the rate constants. C_S and C_z (mg/kg) are the concentrations of ammonium in solution and zeolite, respectively; r is the average radius of zeolite particles (averagely 5×10^{-4} m in this study), t is the contact time (min); and h is the thickness of film around the zeolite particle (10^{-5} m for poorly stirred solution [20]).

The best-fit D_f and D_p values for ammonia adsorption onto the natural and modified zeolites are listed in Table 5. The D_p values for both zeolites were considerably lower than those of D_f, indicating that particle diffusion was the rate-limiting step for ammonium adsorption and the ammonium adsorption was mainly occurred at the surface of zeolite with monolayer molecular adsorption. Similar results were reported by mordenite tests [31] and natural Iranian zeolite [20] at low initial ammonium concentrations. Compared with the natural zeolite, the D_f and D_p values of the modified zeolite increased by 185% and 2.3%, respectively, indicating that NaCl modification could reduce the resistance for mass transfer in film diffusion but have little effects on intra-particle diffusion. Namely, NaCl modification could effectively improve the surface morphology of zeolite particles, but hardly alter the intra-particle structures.

4. Conclusions

In conclusion, this study discloses the mechanisms of ammonium adsorption onto zeolites at different initial ammonium concentrations (10-4000 mg-N/L) and pH levels (3.4-11.1). The ion exchange mechanism dominated the ammonium adsorption process with the order of exchange selectivity for cations: $Na^+ > Ca^{2+} > K^+ > Mg^{2+}$. At initial ammonium concentration > 1000 mg-N/L, Ca^{2+} exceeded Na^+ to dominate the ion exchange process owing to depletion of Na in zeolite. Molecular adsorption occurred at alkaline conditions. NaCl modification enhanced ammonium adsorption capacity from 11.0 to 17.3 mg-N/g (Fig. 6(a)), mainly being contributed by the increased Na contents in zeolite (192%), and by the increased specific surface (32%) and pore diameter (80%) of zeolite, respectively(Table 3). Particle diffusion was the rate-limiting step for the present ammonium adsorption process. The NaCl modification can promote film diffusion significantly through improving the surface characteristics of zeolite.

References:

[1] P.A. Singer, F. Salamanca-Buentello, A.S. Daar, Harnessing Nanotechnology to Improve Global Equity, Issues Sci. Technol. 21 (2005) 57-64.

[2] G.V. Tsitsishvili, T.G. Andronikashvili, G.N. Kirov, L.D. Filizova, Natural zeolites, Ellis Horwood New York, 1992.

[3] M. Kithome, J.W. Paul, L.M. Lavkulich, A.A. Bomke, Kinetics of ammonium adsorption and desorption by the natural zeolite clinoptilolite, Soil Sci. Soc. Am. J. 62 (1998) 622-629.

[4] K. Metropoulos, E. Maliou, M. Loizidou, N. Spyrellis, Comparative-studies between

synthetic and natural zeolites ammonium uptake, J. Environ. Sci. Health, Part A: Toxic/Hazard. Subst. Environ. Eng. 28 (1993) 1507-1518.

[5] L.L. Ames, The cation sieve properties of clinoptilolite, Am. Mineral. 45 (1960) 689-700.

[6] H.M. Huang, X.M. Xiao, B. Yan, L.P. Yang, Ammonium removal from aqueous solutions by using natural Chinese (Chende) zeolite as adsorbent, J. Hazard. Mater. 175 (2010) 247-252.

[7] B.C. Erdogan, S. Ulku, Ammonium sorption by Gordes clinoptilolite rich mineral specimen, Appl. Clay Sci. 54 (2011) 217-225.

[8] L.C. Lei, X.J. Li, X.W. Zhang, Ammonium removal from aqueous solutions using microwave-treated natural Chinese zeolite, Sep. Purif. Technol. 58 (2008) 359-366.

[9] H.B. Wang, Y.M. Bao, J. Zhang, H.Y. Chen, L.Z. Ma, M. Yang, Study on the Preparation and Properties of Na-modified Zeolites, Energy Procedia 11 (2011) 4236-4241.

[10] Z. Liang, J.R. Ni, Improving the ammonium ion uptake onto natural zeolite by using an integrated modification process, J. Hazard. Mater. 166 (2009) 52-60.

[11] S. Balci, Nature of ammonium ion adsorption by sepiolite: analysis of equilibrium data with several isotherms, Water Res. 38 (2004) 1129-1138.

[12] N. Widiastuti, H.W. Wu, H.M. Ang, D.K. Zhang, Removal of ammonium from greywater using natural zeolite, Desalination 277 (2011) 15-23.

[13] S. Ioannidis, A. Anderko, Equilibrium modeling of combined ion-exchange and

molecular adsorption phenomena, Ind. Eng. Chem. Res. 40 (2001) 714-720.

[14] R. Ganigue, H. Lopez, M.D. Balaguer, J. Colprim, Partial ammonium oxidation to nitrite of high ammonium content urban land fill leachates, Water Res. 41 (2007) 3317-3326.

[15] A. Terada, K. Hibiya, J. Nagai, S. Tsuneda, A. Hirata, Nitrogen removal characteristics and biofilm analysis of a membrane-aerated biofilm reactor applicable to high-strength nitrogenous wastewater treatment, J. Biosci. Bioeng. 95 (2003) 170-178.

[16] G. Bujoczek, J. Oleszkiewicz, R. Sparling, S. Cenkowski, High solid anaerobic digestion of chicken manure, J. Agric. Eng. Res. 76 (2000) 51-60.

[17] D. Karadag, Y. Koc, M. Turan, B. Armagan, Removal of ammonium ion from aqueous solution using natural Turkish clinoptilolite, J Hazard. Mater. 136 (2006) 604-609.

[18] APHA, AWWA, WEF, Standard Methods for the Examination of Water & Wastewater, 21st ed., Washington, DC, 2005.

[19] M. Alkan, M. Dogan, Y. Turhan, O. Demirbas, P. Turan, Adsorption kinetics and mechanism of maxilon blue 5G dye on sepiolite from aqueous solutions, Chem. Eng. J. 139 (2008) 213-223.

[20] G. Moussavi, S. Talebi, M. Farrokhi, R.M. Sabouti, The investigation of mechanism, kinetic and isotherm of ammonia and humic acid co-adsorption onto natural zeolite, Chem. Eng. J. 171 (2011) 1159-1169.

[21] Y.F. Wang, F. Lin, W.Q. Pang, Removal of ammonium ions from wastewater using modified zeolites, Fresen. Environ. Bull. 16 (2007) 24-28.

[22] A.M. Yusof, L.K. Keat, Z. Ibrahim, Z.A. Majid, N.A. Nizam, Kinetic and equilibrium studies of the removal of ammonium ions from aqueous solution by rice husk ash-synthesized zeolite Y and powdered and granulated forms of mordenite, J. Hazard. Mater. 174 (2010) 380-385.

[23] F.G. Helfferich, Ion exchange, Dover Pubns, New York, 1995.

[24] V.J. Inglezakis, The concept of "capacity" in zeolite ion-exchange systems, J. Colloid. Interf. Sci. 281 (2005) 68-79.

[25] Y. Watanabe, H. Yamada, H. Kokusen, J. Tanaka, Y. Moriyoshi, Y. Komatsu, Ion exchange behavior of natural zeolites in distilled water, hydrochloric acid, and ammonium chloride solution, Sep. Sci. Technol. 38 (2003) 1519-1532.

[26] N. Kantiranis, K. Sikalidis, A. Godelitsas, C. Squires, G. Papastergios, A. Filippidis, Extra-framework cation release from heulandite-type rich tuffs on exchange with NH_4^+, J. Environ. Manage. 92 (2011) 1569-1576.

[27] D.L. Ford, R.L. Churchwell, J.W. Kachtick, Comprehensive analysis of nitrification of chemical processing wastewaters, J. Water Pollut. Control Fed. (1980) 2726-2746.

[28] Q. Du, S.J. Liu, Z.H. Cao, Y.Q. Wang, Ammonia removal from aqueous solution using natural Chinese clinoptilolite, Sep. Purif. Technol. 44 (2005) 229-234.

[29] V. Vadivelan, K.V. Kumar, Equilibrium, kinetics, mechanism, and process design for the sorption of methylene blue onto rice husk, J. Colloid Interf. Sci. 286 (2005) 90-100.

[30] S.J. Allen, G. Mckay, K. Khader, Intraparticle diffusion of a basic dye during adsorption onto sphagnum peat, Environ. Pollut. 56 (1989) 39-50.

[31] M. Sprynskyy, M. Lebedynets, R. Zbytniewski, J. Namiesnik, B. Buszewski, Ammonium removal from aqueous solution by natural zeolite, Transcarpathian mordenite, kinetics, equilibrium and column tests, Sep. Purif. Technol.46 (2005) 155-160.

Tables

Table 1

Experimental conditions for zeolite adsorption.

No.	Main factor concerned	Experimental conditions					
		Zeolite type	Initial ammonium (mg-N/L)	Temperature (°C)	Agitation speed (rpm)	Time (min)	pH*
1	Temperature	Natural	1000	25, 35, 45	100	15-1440	original
2	Agitation speed	Natural	1000	35	0, 50, 100, 200	15-1440	original
3	Initial ammonium concentration	Natural	10-4000	35	100	1440	original
4	pH	Natural	100 / 1000	35	100	1440	3.4-11.1
5	Contact time	Natural / Modified	1000	35	100	15-1440	original

(*The original pH of 100 and 1000 mg-N/L of ammonium chloride solution were 6.68 and 5.38, respectively)

Table 2

Chemical compositions of the natural and modified zeolites before and after ammonium adsorption under 1000 mg-N/L of initial ammonium concentration by EDS (wt%).

Chemical elements	Before adsorption		After adsorption	
	Natural	Modified	Natural	Modified
O	42.73	40.78	48.69	45.98
Na	1.61	4.70	0.49	0.59
Mg	0.87	0.35	0.35	0.38
Al	11.00	9.63	9.63	6.87
Si	37.22	41.33	38.18	43.81
K	1.52	1.48	0.84	1.40
Ca	2.09	0.45	0.77	0.20
Others	2.96	1.28	1.05	0.77

Table 3

Information of surface area and pore size for the natural and modified zeolites by BET (at $P/P_0 \geq 0.995$).

	Unit	Zeolite type	
		Natural	Modified
BET surface area	m^2/g	14.33	60.83
Total pore volume	cm^3/g	0.044	0.065
Average pore diameter	nm	16.19	29.24

Table 4

Isotherms constants for ammonium adsorption onto the natural zeolite.

Langmuir parameters			Freundlich parameters		
q_{max}(mg-N/g)	K_L	R^2	K_F	$1/n$	R^2
14.265	0.009	0.993	0.985	0.355	0.973

Table 5

Kinetic constants for ammonium adsorption onto the natural and modified zeolites.

Models		Parameters	Zeolite type	
			Natural	Modified
Intra-particle diffusion model	First stage	k_{d1}	0.797	1.561
		R^2	0.984	0.916
	Second stage	k_{d2}	0.095	0.173
		R^2	0.815	0.877
Film diffusion model		D_f (m^2/s)	8.422×10^{-10}	24.021×10^{-10}
		R^2	0.966	0.855
Particle diffusion model		D_p (m^2/s)	5.700×10^{-11}	5.832×10^{-11}
		R^2	0.974	0.988

Figure captions

Fig. 1. XRD patterns of the natural and modified zeolites.

Fig. 2. SEM images of the natural (a) and modified zeolites (b).

Fig. 3. Effects of agitation speed and temperature on ammonium adsorption by natural zeolite under 1000 mg-N/L of initial ammonium concentration condition. (a) Effect of agitation speed under 35°C, (b) Effect of temperature under 100 rpm.

Fig. 4. The ions release and ammonium adsorption capacity of natural zeolite under different initial ammonium concentration conditions.

Fig. 5. Effect of pH on ammonium and ammonia removal by natural zeolite under initial ammonium concentration of 100 mg-N/L and 1000 mg-N/L, respectively (35°C).

Fig. 6. Kinetic results of ammonium adsorption onto the natural and modified zeolites under 1000 mg-N/L of initial ammonium concentration condition. (a) Effect of contact time, (b) Kinetic plots of intra-particle diffusion model.
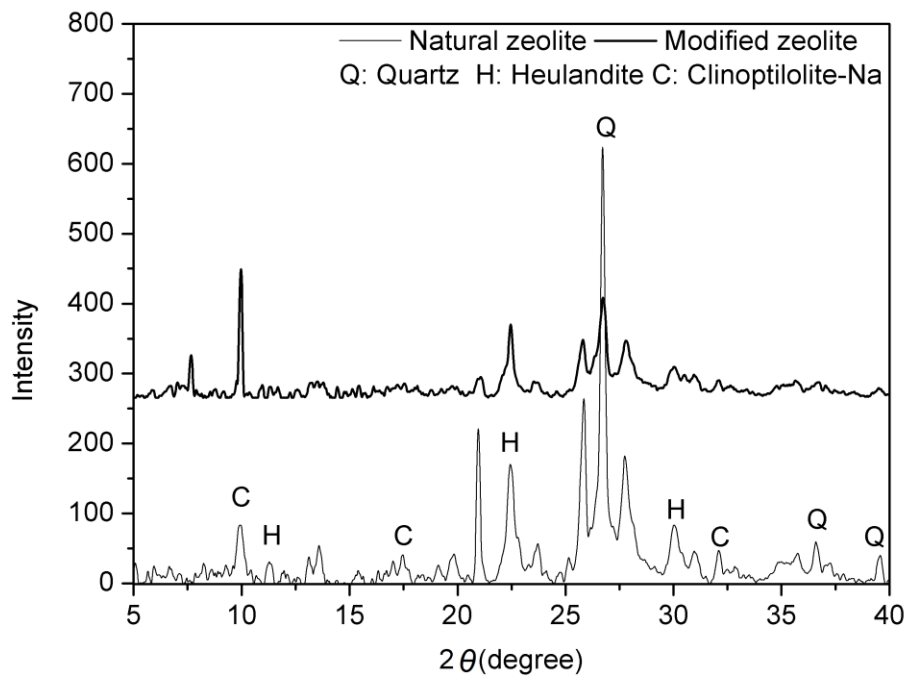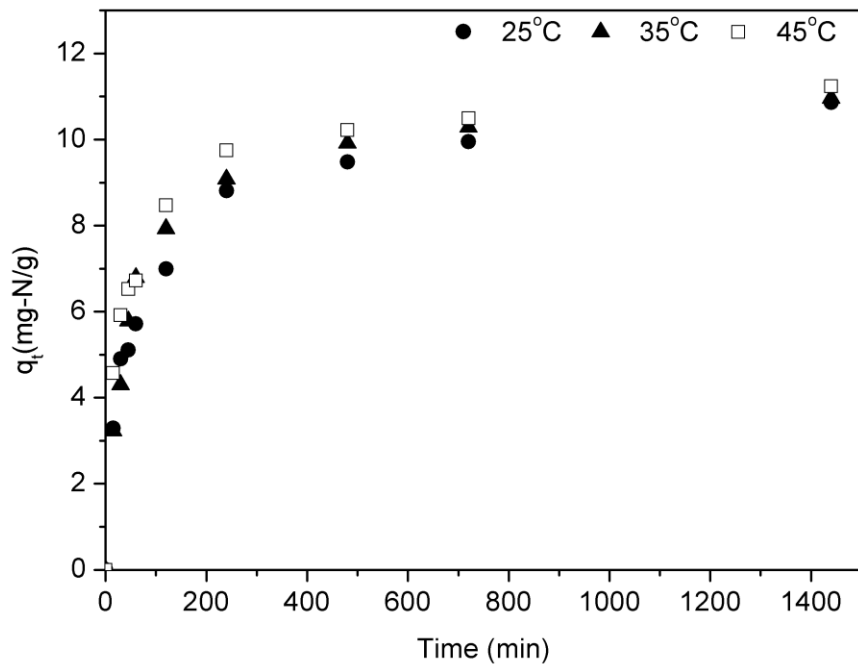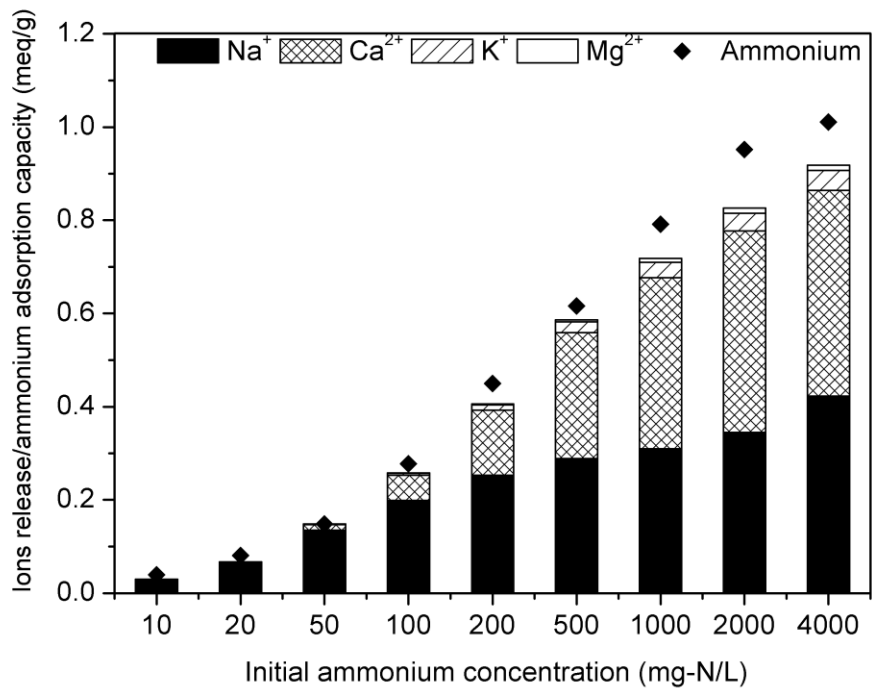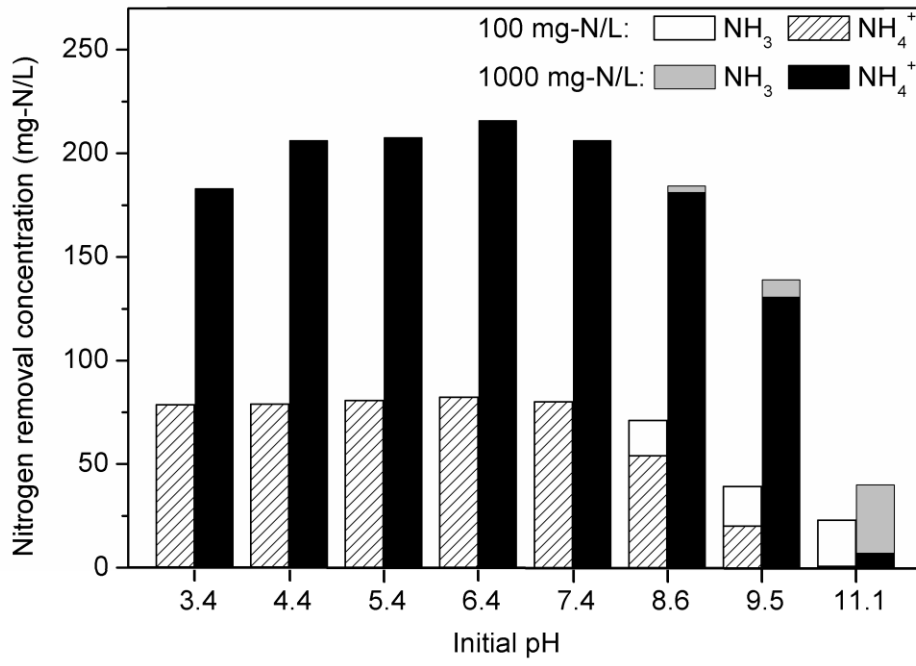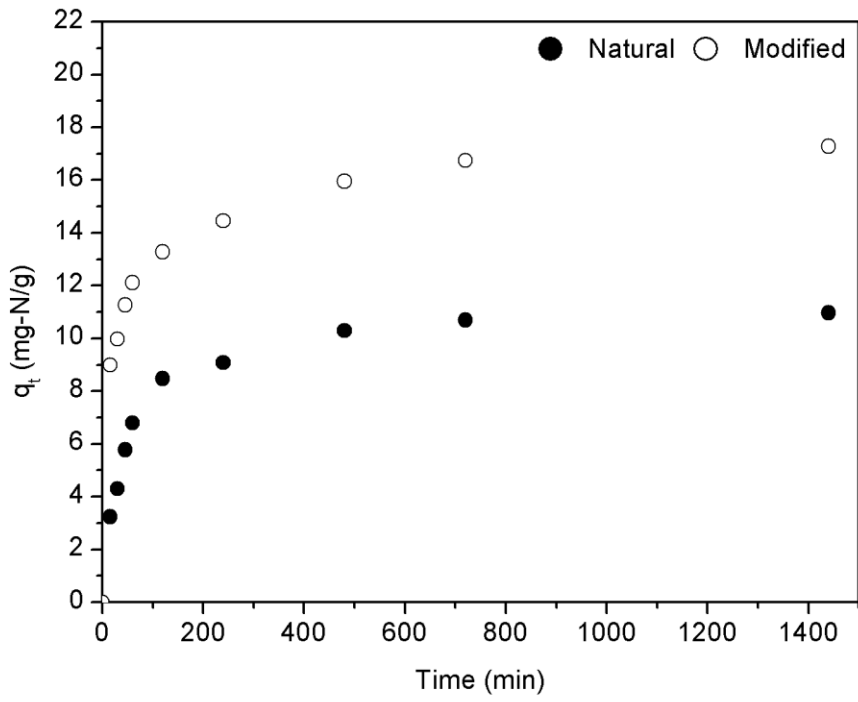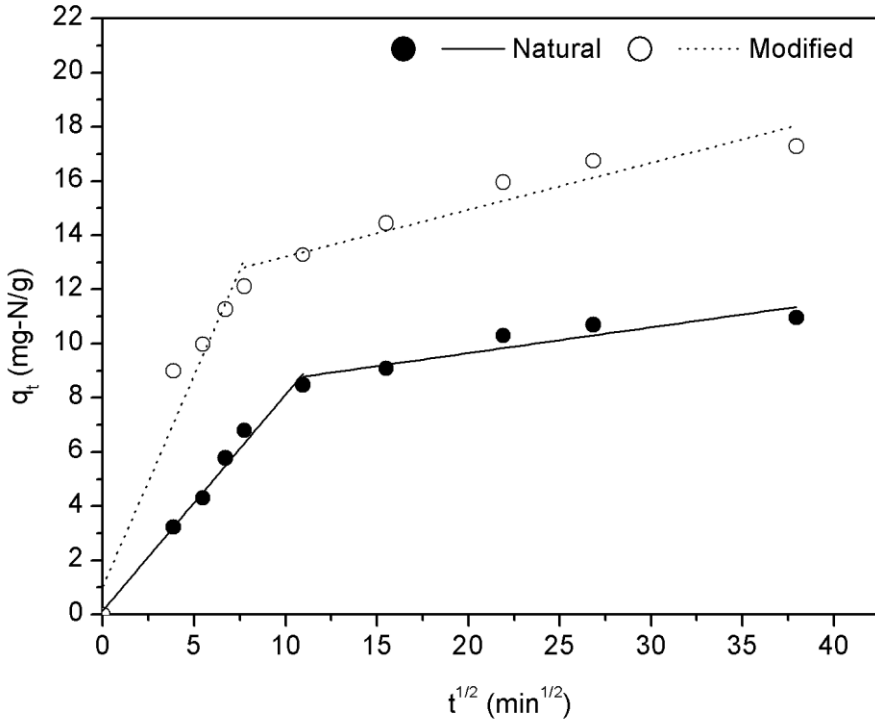
Fig. 1
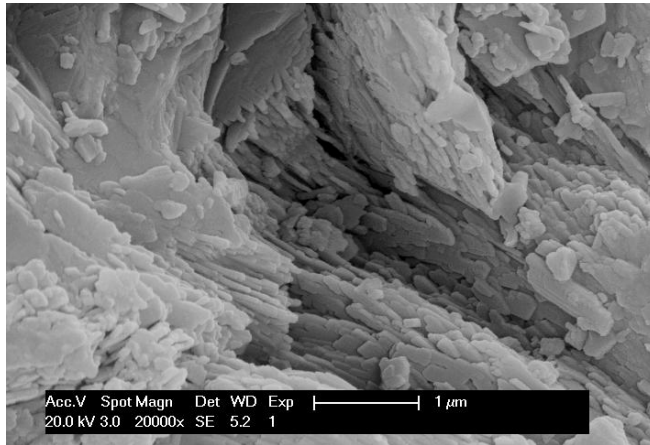
Fig. 2(a)
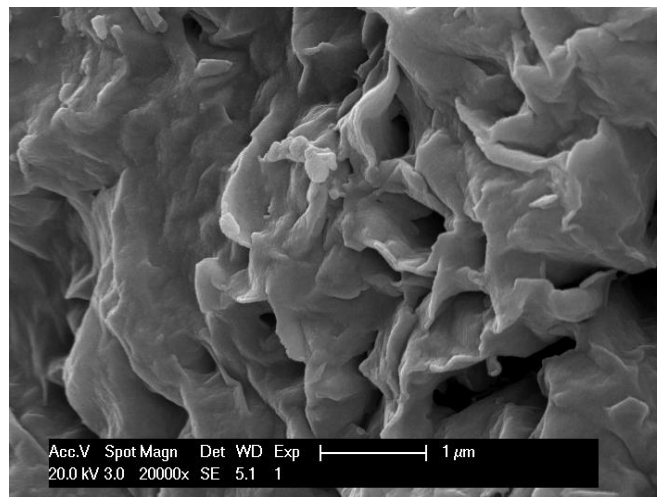
Fig. 2(b)
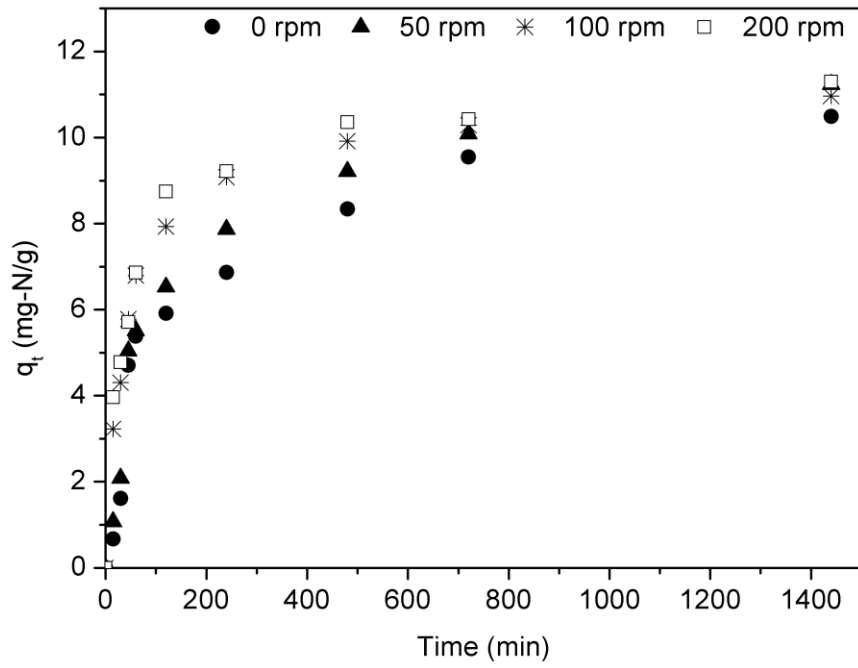
Fig. 3(a)

Fig. 3(b)

Fig. 4

Fig. 5

Fig. 6(a)

Fig. 6(b)